seals. Although the two harbor seals with proven influenza B virus infection displayed respiratory symptoms during their rehabilitation period, this occurred at a time when many of the admitted juvenile seals suffered from lungworm (*Otostrongylus circumlitus* and *Parafilaroides gymnurus*) infections (*17*). Association of lungworm infections in pigs with influenza A virus pathogenesis and transmission has been described (*25*), but the evidence was considered weak (*26*).

The combined serological and virological data obtained from seal 99-012 indicate that shedding of influenza B virus in seals was prolonged as compared to shedding in humans (*27, 28*) and that IgG antibody responses to NP and HA/NA were delayed. Possible explanations for this apparent suboptimal immune response upon infection may be associated with xenobiotic-related immunosuppression (*11*) or the therapeutic use of corticosteroids to combat the lungworm infections (*17*). Prolonged virus shedding in addition to the limited spreading of influenza B virus among seals (as shown in the SRRC and indicated by the limited seroprevalence of specific antibodies in the wild) may explain why little or no genetic and antigenic drift of influenza B virus is observed in seals.

Our data not only highlight the fact that influenza B virus infections can emerge in seal populations but also show that seals may constitute an animal reservoir from which humans may be exposed to influenza B viruses that have circulated in the past.

References and Notes

1. B. R. Murphy and R. G. Webster, in *Virology*, B. N. Fields *et al.*, Eds. (Raven, New York, 1990).
2. R. G. Webster, W. J. Bean, O. T. Gorman, T. M. Chambers, Y. Kawaoka, *Microbiol. Rev.* **56**, 152 (1992).
3. C. P. Chang, A. E. New, J. F. Taylor, H. S. Chiang, *Int. J. Zoon.* **3**, 61 (1976).
4. G. Takatsy, J. Romvary, E. Farkas, *Acta Microbiol. Acad. Sci. Hung.* **14**, 309 (1967).
5. C. M. Prato, T. G. Akers, A. W. Smith, *Nature* **249**, 255 (1974).
6. A. W. Smith and D. E. Skilling, *J. Am. Vet. Med. Assoc.* **175**, 918 (1979).
7. A. D. Osterhaus *et al.*, *Arch. Virol.* **86**, 239 (1985).
8. A. D. Osterhaus and E. J. Vedder, *Nature* **335**, 20 (1988).
9. A. D. Osterhaus *et al.*, *Nature* **337**, 21 (1989).
10. A. D. Osterhaus *et al.*, *Nature* **388**, 838 (1997).
11. C. D. Harvell *et al.*, *Science* **285**, 1505 (1999).
12. J. R. Geraci *et al.*, *Science* **215**, 1129 (1982).
13. V. S. Hinshaw *et al.*, *J. Virol.* **51**, 863 (1984).
14. R. G. Webster *et al.*, *Virology* **113**, 712 (1981).
15. R. J. Callan, G. Early, H. Kida, V. S. Hinshaw, *J. Gen. Virol.* **76**, 199 (1995).
16. G. F. Rimmelzwaan, M. Baars, E. C. Claas, A. D. Osterhaus, *J. Virol. Methods* **74**, 57 (1998).
17. A. D. Osterhaus, G. F. Rimmelzwaan, B. E. Martina, T. M. Bestebroer, R. A. Fouchier, unpublished data.
18. RNA was isolated by means of a high pure RNA isolation kit (Boehringer-Mannheim). RNA was used for RT-PCR analysis to amplify a 240–base pair fragment of the influenza B virus *NS* gene segment using primers 5′-ATG GCC ATC GGA TCC TCA AC-3′ and 5′-TGT CAG CTA TTA TGG AGC TG-3′, and AMV reverse transcriptase, Amplitaq DNA polymerase, recombinant ribonuclease inhibitor (Promega) in the presence of 50 mM tris-HCl, 50 mM NaCl, 2 mM dithiothreitol, 7 mM $MgCl_2$, 1 mM dNTP, and 400 nM each of primer. Cycling parameters were 30 min at 42°C, 4 min at 95°C, 1 min at 45°C, and 3 min at 72°C once; and then 1 min at 95°C, 1 min at 45°C, and 3 min at 72°C, repeated 39 times. PCR fragments were sequenced with a DYEnamic ET terminator cycle sequencing premix kit (Amersham) on an ABI-373A apparatus (Perkin Elmer).
19. Seal kidney cells were plated in Dulbecco's modified Eagle's medium (DMEM) supplemented with 10% fetal bovine serum, 1% L-glutamine, penicillin, and streptomycin at 1×10^5 cells per well in 24-well plates. Cells were inoculated with 1×10^5 $TCID_{50}$ of influenza virus B/Seal/Netherlands/1/99 in DMEM supplemented with 4% bovine serum albumin, 1% L-glutamine, penicillin, and streptomycin. Influenza B virus infection was detected by immunofluorescence with influenza B NP-specific antibodies, which were labeled with fluorescein isothiocyanate (IMAGEN Influenza A+B, DAKO Diagnostics) after 24 hours. Cytopathic changes and HA activity (titer = 32) were detected in the culture cell after 48 hours.
20. J. T. Voeten *et al.*, *J. Clin. Microbiol.* **36**, 3527 (1998).
21. Antibody titers were determined with a recombinant fusion protein between maltose-binding protein (MBP) and NP or with HA/NA proteins purified from virions (both proteins were derived from B/Harbin/7/94). IgG antibody levels to HA/NA and NP proteins were determined by an indirect ELISA with antigen-coated plates and peroxidase-labeled protein A for detection. IgM antibody levels to NP were determined by means of an antibody-capture ELISA with goat anti-dog IgM–coated plates and peroxidase-labeled MBP-NP antigen for detection. The goat anti-dog IgM antibody preparation specifically captures seal IgM, as was shown in routine serological tests for PDV and PHV.
22. I. M. Roitt, *Essential Immunology* (Blackwell Scientific, Oxford, ed. 8, 1994).
23. The sequences of influenza B virus *HA* and *NS* genes are available at www.flu.lanl.gov/.
24. Analysis of the *HA1* sequences from human influenza B virus strains that are available from the influenza sequence database showed that between 1991 and 1999, the proportion of strains with >98% nucleotide identity to B/Seal/Netherlands/1/99 was 0, 17, 27, 46, 62, 29, 0, 0, and 0% of all epidemic strains for each successive year, respectively.
25. R. E. Shope, *J. Exp. Med.* **77**, 111 (1943).
26. G. D. Wallace, *J. Infect. Dis.* **135**, 490 (1977).
27. A. L. Frank *et al.*, *J. Infect. Dis.* **144**, 443 (1981).
28. C. B. Hall, R. G. Douglas, J. M. Geiman, M. P. Meagher, *J. Infect. Dis.* **140**, 610 (1979).
29. *HA1* sequences were amplified with M13-tagged primers P1 (5′-29M13-GCA TTT TCT AAT ATC CAC AA-3′) and P4 (5′-21M13-TTT GGG AAG CCA CCA ATC TG-3′) or primers P3 (5′-29M13-CCT ATA ATG CAC GAC AGA AC-3′) and P6 (5′-21M13-AAA CCA GCA ATA GCT CCG AA-3′), followed by sequencing with primers 29M13 (5′-CAG GAA ACA GCT ATG ACC-3′) and 21M13 (5′-TGT AAA ACG ACG GCC AGT-3′) using a DYEnamic ET terminator cycle sequencing premix kit (Amersham) and an ABI-373A sequencing apparatus (Perkin Elmer).

30. We are grateful to L. van der Kemp, G. de Mutsert, and M. van der Bildt for technical assistance; J. Habova for electron microscopy; Solvay Pharmaceuticals, Weesp, the Netherlands, for providing HA/NA proteins from B/Harbin/7/94; and the SRRC staff for taking care of and samples from seals. R. F. is a fellow of the Royal Netherlands Academy of Arts and Sciences.

13 January 2000; accepted 6 March 2000

Noxa, a BH3-Only Member of the Bcl-2 Family and Candidate Mediator of p53-Induced Apoptosis

Eri Oda,[1]* Rieko Ohki,[1]* Hideki Murasawa,[1] Jiro Nemoto,[1] Tsukasa Shibue,[1] Toshiharu Yamashita,[2] Takashi Tokino,[2] Tadatsugu Taniguchi,[1]† Nobuyuki Tanaka[1]

A critical function of tumor suppressor p53 is the induction of apoptosis in cells exposed to noxious stresses. We report a previously unidentified pro-apoptotic gene, *Noxa*. Expression of Noxa induction in primary mouse cells exposed to x-ray irradiation was dependent on p53. *Noxa* encodes a Bcl-2 homology 3 (BH3)–only member of the Bcl-2 family of proteins; this member contains the BH3 region but not other BH domains. When ectopically expressed, Noxa underwent BH3 motif–dependent localization to mitochondria and interacted with anti-apoptotic Bcl-2 family members, resulting in the activation of caspase-9. We also demonstrate that blocking the endogenous Noxa induction results in the suppression of apoptosis. Noxa may thus represent a mediator of p53-dependent apoptosis.

The mechanism of p53-induced apoptosis has been extensively studied in the context of tumor suppression (*1*). p53-dependent apoptosis is regulated, at least in part, by transcriptional activation of its target genes (*1*), and this process is dependent on the Apaf-1/caspase-9 activation pathway (*2*). Among the identified target genes of p53, *Bax* encodes a pro-apoptotic Bcl-2 family of proteins that can activate this pathway (*3*). However, in *Bax*-deficient mice, DNA damage–induced apoptosis occurs normally in thymocytes, and apoptosis induced by treatment with anticancer drugs is only partly inhibited in mouse embryo fibroblasts (MEFs) expressing the adenovirus oncoprotein E1A (*4*). Furthermore, thymocytes from *p53*-defi-

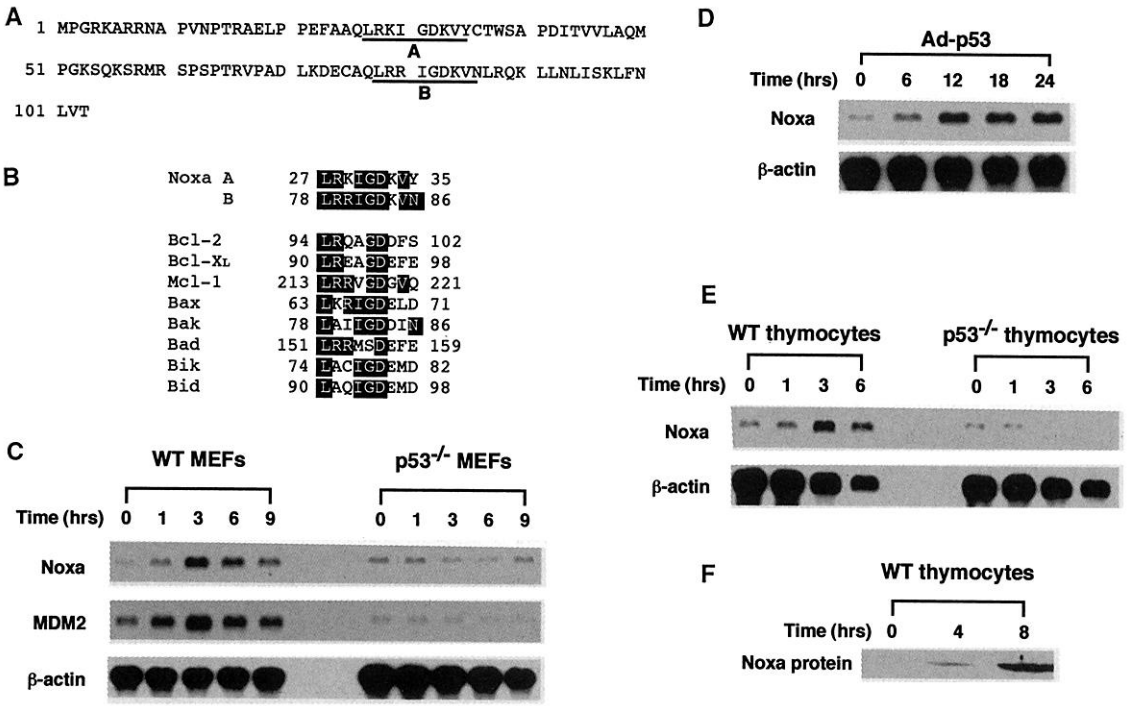

Fig. 1. Primary sequence of Noxa and its expression. (**A**) Predicted amino acid sequence of Noxa (*28*). Two putative BH3 motifs are underlined (regions A and B). (**B**) Alignment of the Noxa BH3 motifs with the BH3 domains of Bcl- 2 family proteins; anti-apoptotic Bcl-2 subfamily proteins (human Bcl-2, GenBank accession number M14745; human Bcl-XL, GenBank accession number Z23115; human Mcl-1, GenBank accession number Q07820), pro-apoptotic Bax subfamily proteins (human Bax, GenBank accession number L22473; human Bak, GenBank accession number U23765), and pro-apoptotic BH3-only subfamily proteins (mouse Bad, GenBank accession number L37296; human Bik, GenBank accession number U34584; mouse Bid, GenBank accession number U75506). Amino acids identical to Noxa's BH3 motifs are shaded. (**C**) Expression of Noxa mRNA following x-ray irradiation in MEFs. Noxa mRNA was analyzed by RNA blotting with RNAs (5 μg in each lane) isolated from wild-type (WT) and *p53*-deficient ($p53^{-/-}$) MEFs following x-ray irradiation [20 grays (Gy)]; time after radiation is indicated in hours. The same filter was probed with MDM2 or β-actin cDNA. (**D**) Expression of Noxa mRNA in $p53^{-/-}$ MEFs following p53 expression. Cells were infected with p53-expressing adenovirus (Ad-p53) for the indicated time periods, and RNA blotting was performed as in (C). The same filter was probed with β-actin cDNA. (**E**) Expression of Noxa mRNA in thymocytes following x-ray irradiation. Noxa mRNA was analyzed by RNA blotting with RNAs (5 μg in each lane) isolated from WT and $p53^{-/-}$ thymocytes following x-ray irradiation (5 Gy). The same filter was probed with β-actin cDNA. (**F**) Expression of Noxa protein. Noxa protein was determined by immunoblot analysis with antibody to Noxa in WT thymocytes following x-ray irradiation (5 Gy); time after radiation is indicated.

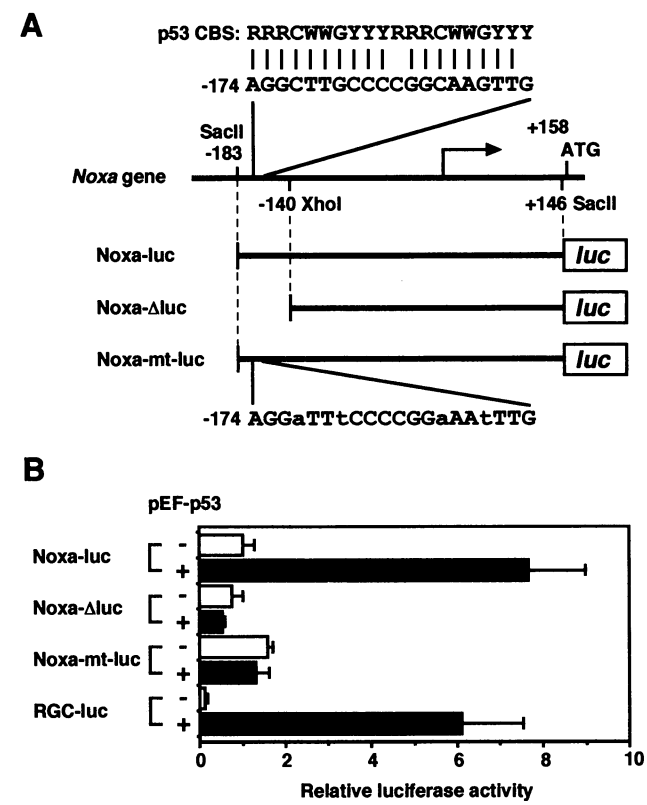

Fig. 2. Activation of the *Noxa* promoter by p53. (**A**) The *Noxa* promoter and luciferase reporter gene constructs. Putative p53-recognition sequence and p53-consensus binding sequence (p53 CBS) are shown. The following reporter plasmids using this assay are also indicated: Noxa-luc containing Noxa promoter and putative p53-recognition sequence, Noxa-Δluc lacking putative p53-recognition sequence, and Noxa-mt-luc in which four critical nucleotide residues for p53 binding were altered (indicated by lowercase letters). (**B**) Transient cotransfection analysis of p53. p53 expression vector (pEF-p53) (0.05 μg) was transfected into 8×10^4 $p53^{-/-}$ MEFs with 0.2 μg of each reporter plasmid. Luciferase activity was measured 24 hours after transfection. RGC-luc (*29*) containing synthetic p53-binding sequences was used as a positive control. Histogram shows the mean of three independent experiments, and error bars show standard deviations. The assay was repeated three times, and the results were reproducible.

cient mice with a *Bax* transgene nevertheless showed resistance similar to that of thymocytes without the transgene to DNA damage–induced apoptosis (*5*). Therefore, the existence of at least one other target gene appears to be necessary to explain the full p53-dependent apoptotic response.

p53 and interferon regulatory factor–1 (IRF-1), a critical transcription factor in the interferon response, cooperate in tumor suppression and in regulation of the cell cycle and apoptosis (*6*). These observations prompted us to search for target genes of IRF-1, p53, or both that show increased transcription in response to DNA damage. We used a mRNA differential display method (*7*) to isolate cDNAs whose mRNA expression profiles differed between the x-ray–irradiated wild-type and *IRF-1/p53* doubly deficient MEFs. We identified a gene termed *Noxa* (for *damage*). Its cDNA encodes a 103–amino acid protein (Fig. 1A), and it lacks any known motif except for two mutually related

[1]Department of Immunology, Graduate School of Medicine and Faculty of Medicine, University of Tokyo, Hongo 7-3-1, Bunkyo-ku, Tokyo 113-0033, Japan. [2]Department of Molecular Biology, Cancer Research Institute, Sapporo Medical University School of Medicine, S1 W17, Chuo-Ku, Sapporo 060-8543, Japan.

*These authors contributed equally to this report.
†To whom correspondence should be addressed. E-mail: tada@m.u-tokyo.ac.jp

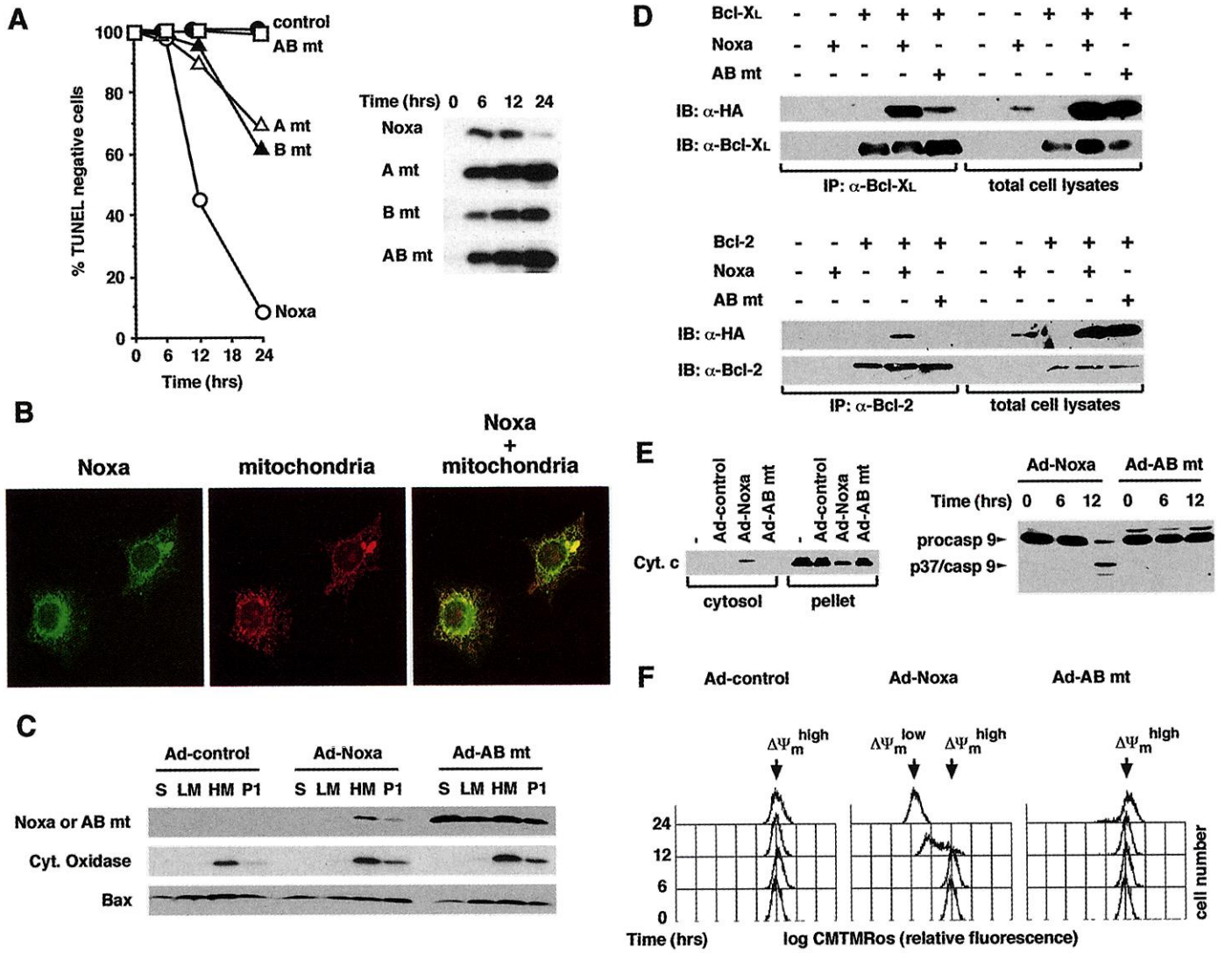

Fig. 3. Functional characterization of Noxa. (**A**) Induction of apoptosis by Noxa and the effect of mutations in its BH3 motifs. HeLa cells were infected with control adenovirus (control) (solid circles), adenovirus expressing Noxa (Noxa) (open circles), and adenoviruses expressing a mutant form of Noxa: A mt (open triangles), B mt (solid triangles), and AB mt (squares). Percentage of TUNEL-negative cells was determined at the indicated times in hours (left). One of two similar results is shown. The expression of Noxa and its mutant proteins in the same cells was determined by immunoblot analysis with antibody to HA at the indicated time (right). (**B**) Subcellular localization of Noxa protein. Twelve hours after infection in HeLa cells by adenovirus expressing Noxa, the HA-tagged Noxa protein was stained with antibody to HA (green), and mitochondria were stained with CMTMRos (red) (Molecular Probes); the two images were overlaid (Noxa + mitochondria) by confocal laser microscopy (μRadiance, Bio-Rad). (**C**) Subcellular distribution of the Noxa protein. HeLa cells infected with adenovirus expressing Noxa (Ad-Noxa) for 12 hours were separated into cytosol (soluble fraction, S), plasma membrane (light membrane fraction, LM), mitochondria-rich (heavy membrane fraction, HM), and nuclear (containing nuclei and some mitochondria) (low-speed pellet, P1) fractions. All fractions were adjusted to the same volume and analyzed by immunoblotting with antibodies to HA (Noxa), cytochrome oxidase subunit IV (Cyt. Oxidase) (as a mitochondrial marker), and Bax. Ad-control, control adenovirus; Ad-AB mt, adenovirus expressing mutant forms of Noxa. (**D**) Noxa protein is associated with Bcl-XL and Bcl-2. HeLa cells were transfected with Bcl-XL or Bcl-2 expression vectors (pEF-Bcl-XL or pEF-Bcl-2, respectively). After 36 hours, these cells infected with Ad-Noxa or Ad-AB mt for 12 hours. Cell extracts were immunoprecipitated (IP) with antibodies to Bcl-XL (α-Bcl-XL) or Bcl-2 (α-Bcl-2) and subjected to immunoblot (IB) analysis with antibodies to HA (α-HA), Bcl-XL, or Bcl-2. Essentially identical results were obtained when the same extracts were analyzed by IB with α-Bcl-XL followed by IP with α-HA. Ectopically expressed protein is indicated as +. (**E**) Cytochrome c release and caspase-9 activation by Noxa. Cytosolic extracts were prepared from HeLa cells that were mock-infected (−), or they were prepared 12 hours after infection with the indicated adenoviruses. Cytosolic extracts (cytosol) and extracts from the residual pelleted fraction (pellet) were subjected to immunoblot analysis using antibody cytochrome c (Cyt. c) (left). Caspase-9 activation was determined with extracts from HeLa cells at the indicated time after infection with Ad-Noxa or Ad-AB mt by immunoblot analysis with antibody to caspase-9 (right). The unprocessed caspase-9 precursor (procasp 9) and the cleaved 37-kD product of active caspase-9 (p37/casp 9) are indicated. (**F**) Reduction in ΔΨm by Noxa. ΔΨm was measured by fluorescence of the cationic lipophilic dye CMTMRos with a flow cytometer at the indicated time after infection with Ad-control, Ad-Noxa, and Ad-AB mt. A reduction in ΔΨm is observed as "ΔΨm low." The reduction was inhibited by the addition of a caspase inhibitor, z-VAD fmk, suggesting that the permeability change may be a postcaspase event (*9*).

9–amino acid sequences (A and B) characteristic to the Bcl-2 homology 3 (BH3) motif of the Bcl-2 family of proteins (Fig. 1B) (*8*).

Noxa mRNA was constitutively expressed in small amounts in the brain, thymus, spleen, lung, kidney, and testis of adult mice (*9*). X-ray irradiation of wild-type MEFs increased expression of Noxa mRNA about fivefold (Fig. 1C), with kinetics similar to those of the p53-depen-

dent gene *MDM2* (*1*). In contrast, expression of the *Noxa* gene was totally abolished in *p53*-deficient MEFs but not in *IRF-1*–deficient MEFs (Fig. 1C) (*9, 10*). Moreover, ectopic expression of p53 resulted in increased expression of Noxa mRNA in *p53*-deficient MEFs (Fig. 1D). Thymocytes undergo DNA damage–induced apoptosis in a p53-dependent manner (*11*). Increased expression of Noxa mRNA in response to x-ray irradiation also occurred in wild-type thymocytes (fivefold increase) but not in *p53*-deficient thymocytes (Fig. 1E). Noxa protein also accumulated in wild-type thymocytes after x-ray irradiation (Fig. 1F) (*12*).

To determine whether the p53-dependent expression of the *Noxa* gene involves direct activation of its promoter, we isolated and characterized the mouse *Noxa* gene (*13*). This gene contains three exons in which the BH3 motifs A and B are encoded by exons 2 and 3, respectively. The transcription initiation site was determined to be 158 base pairs upstream from the initiator ATG by polymerase chain reaction (PCR)–based primer extension, and one potential p53-recognition sequence, located at −155 to −174, was found in the promoter region (Fig. 2A). The contribution of p53 to the activation of the *Noxa* promoter was examined by a transient cotransfection assay using a *luciferase* reporter gene linked to *Noxa* promoter (Noxa-luc in Fig. 2A) (*14*). The promoter was activated (on average, sevenfold) by coexpressed p53 in *p53*-deficient MEFs. In contrast, reporter genes containing a deletion (Noxa-Δluc) or point mutations (Noxa-mt-luc) in the putative p53-recognition sequence were not activated by p53 (Fig. 2B). Collectively, these results lend support to the idea that expression of the *Noxa* gene in x-ray–irradiated cells involves direct activation of its promoter by p53.

On the basis of its retention of various BH domains, the Bcl-2 family can be divided into three classes: the anti-apoptotic Bcl-2, the pro-apoptotic Bax, and BH3-only subfamilies (*8*). The BH3 domain of the pro-apoptotic members is critical for association with other Bcl-2 family proteins in the promotion of apoptosis (*8*). Unlike Bax, whose expression is also regulated by p53 (*3*), Noxa contains BH3 but not other BH motifs (BH1, BH2, and BH4) or a transmembrane domain; hence, it appears be a previously unknown member of the BH3-only subfamily. Ectopic expression of Noxa in HeLa cells with an adenovirus-mediated gene expression system caused apoptosis in >90% of the cells 24 hours after virus infection (Fig. 3A) (*15*). This Noxa-induced apoptosis was also observed in other human cancer cell lines independently of their p53 status (*9*). Because substitution of the NH_2-terminal leucine to alanine in the BH3 domain of another BH3-only member, Bad, is known to cause a loss of pro-apoptotic activity (*16*), we generated mutant Noxa cDNAs in which one amino acid substitution was similarly introduced in either or both of the leucine residues within the BH3 motifs (*15*). Noxa mutants carrying one substitution (A mt and B mt) had lower pro-apoptotic activities than wild-type Noxa, and the mutant carrying both substitutions (AB mt) was totally inactive (Fig. 3A). Thus, the BH3 motifs are central to Noxa's pro-apoptotic activity. Noxa-induced apoptosis was suppressed by co-expression of the anti-apoptotic members of the Bcl-2 family, Bcl-XL or Bcl-2 (*9*).

We examined subcellular localization of

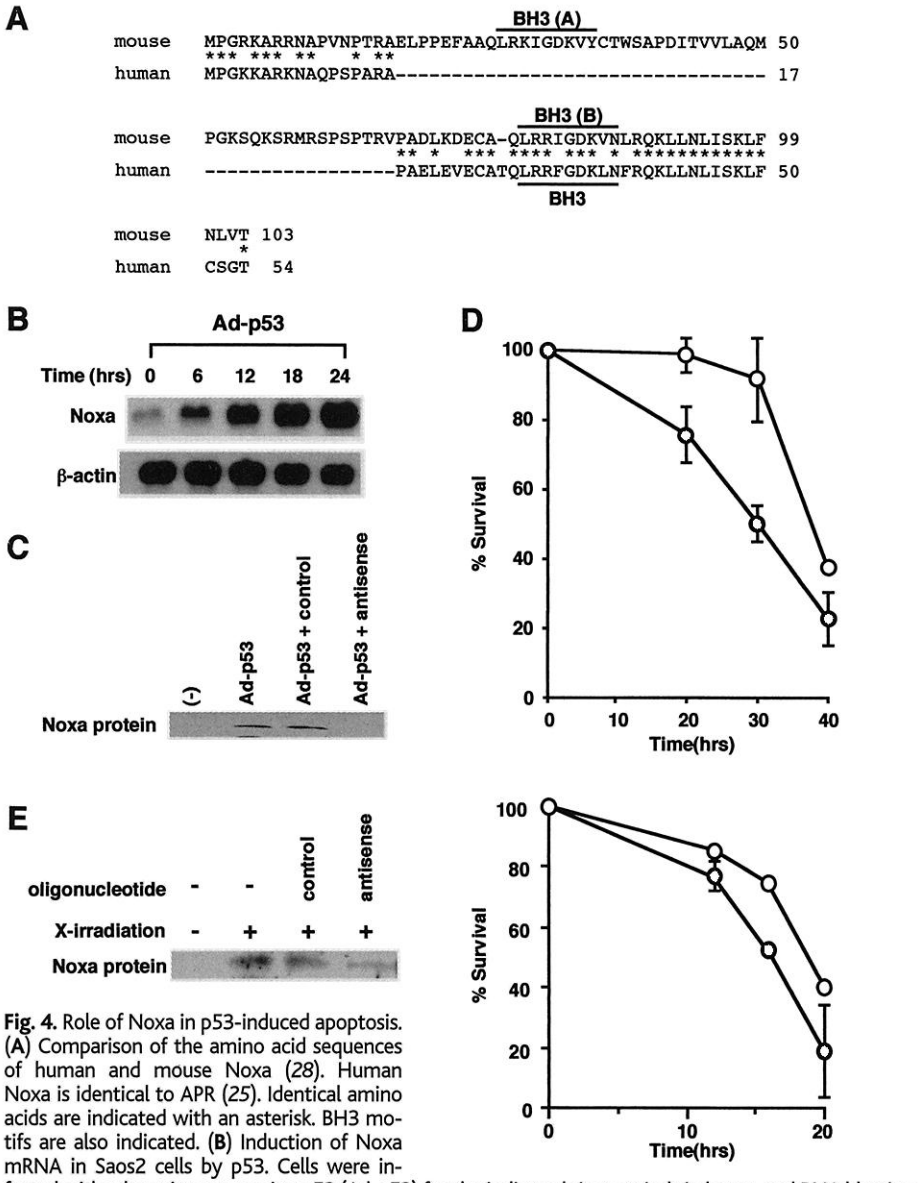

Fig. 4. Role of Noxa in p53-induced apoptosis. (**A**) Comparison of the amino acid sequences of human and mouse Noxa (*28*). Human Noxa is identical to APR (*25*). Identical amino acids are indicated with an asterisk. BH3 motifs are also indicated. (**B**) Induction of Noxa mRNA in Saos2 cells by p53. Cells were infected with adenovirus expressing p53 (Ad-p53) for the indicated time periods in hours, and RNA blotting was performed. The same filter was probed with β-actin cDNA. (**C**) Reduction of endogenous Noxa protein by transfection with Noxa antisense oligonucleotide. Noxa protein was determined by immunoblot analysis with antibody to human Noxa in Saos2 cells 20 hours after infection with Ad-p53 following transfection with 4 μM antisense (Ad-p53 + antisense) or control (Ad-p53 + control) oligonucleotide for 4 hours. Noxa protein was also determined before (−) and after infection with Ad-p53 (Ad-p53) for 20 hours without oligonucleotides. (**D**) Effect of Noxa antisense oligonucleotide in p53-induced apoptosis. Saos2 cells were transfected with antisense (open circles) or control (solid circles) oligonucleotide as in (C) and infected with Ad-p53 for the indicated times. Viable cells were determined by trypan blue exclusion and calculated as the percentage of survival in relation to the number at the start of trial. Error bars represent standard deviations from two independent samples. We tested two other control oligonucleotides and confirmed that these oligonucleotides had no effect. (**E**) Effect of Noxa antisense oligonucleotide in x-ray irradiation–induced apoptosis of BAF-3 cells. BAF-3 cells were incubated with 10 μM antisense or control oligonucleotide for 12 hours and were subjected to x-ray irradiation (4 Gy). Noxa protein was determined by immunoblot analysis with antibody to mouse Noxa 16 hours after x-ray irradiation (+) (−, before infection) in the absence or presence of indicated oligonucleotides (left). Viable cells were determined after irradiation in the presence of antisense (open circles) or control (solid circles) oligonucleotides by trypan blue exclusion and calculated as percentage of survival (right). Error bars represent standard deviations from two independent samples.

epitope-tagged Noxa by immunohistochemical analysis in HeLa cells. Noxa was colocalized with a mitochondrial marker, CMTMRos (Fig. 3B) (*17*). Immunoblot analysis of subcellular fractions also showed that most of the ectopically expressed Noxa protein was located in the mitochondria-rich heavy membrane fraction and a small amount was detected in the low-speed pellet, which contains residual mitochondria together with nuclei (Fig. 3C) (*18*). On the other hand, the Noxa mutant lacking functional BH3 motifs (AB mt) was found in all fractions (Fig. 3C), indicating that the selective localization of Noxa to mitochondria is contingent on its functional BH3 motifs. Bax is known to accumulate in mitochondria in response to death signals (*18, 19*). Endogenous Bax protein was dispersed in all fractions, even after ectopic expression of Noxa (Fig. 3C), and Noxa failed to bind Bax (*9*). Therefore, the function of Noxa is likely to be independent of that of Bax. In fact, BH3-only subfamily members are known to induce apoptosis by association with anti-apoptotic Bcl-2 family members or by stimulating other apoptosis-promoting factors (*8*). Noxa indeed coimmunoprecipitated with coexpressed Bcl-XL or Bcl-2, and this coimmunoprecipitation was dependent on the BH3 motifs of Noxa (Fig. 3D). We also found that endogenous Noxa, induced in irradiated thymocytes, also coimmunoprecipitated with Bcl-XL (*9*). Such an interaction was also observed with another Bcl-2 member, Mcl-1 (*20*), collectively suggesting the selective interaction of Noxa with the anti-apoptotic Bcl-2 subfamily of proteins.

Because p53-dependent apoptosis is dependent on the activation of Apaf-1 and caspase-9 (*2*), we also examined whether Noxa affected these events. Cytochrome c release, which induces Apaf-1 activation (*21*), and caspase-9 activation were also observed in these cells (Fig. 3E). The mitochondrial permeability change is also induced during the process of p53-dependent apoptosis (*22*). A decrease in mitochondrial membrane potential ($\Delta\Psi$m), which is mediated by the opening of the mitochondrial permeability transition pore (*17, 23*), was detected 12 hours after infection of HeLa cells with the Noxa-expressing adenovirus (Fig. 3F).

To examine the involvement of Noxa in p53-induced apoptosis, we used human Saos2 cells, which lack p53 expression (*24*). We screened for a human homolog of Noxa cDNA and found that the cloned cDNA showing the highest degree of similarity is identical to the previously identified human gene *APR* (*25*). However, the function of this gene is not known, and its regulation by p53 has not been demonstrated. Human *Noxa*, or *APR*, encodes 54 amino acids, containing only one BH3 motif at amino acids 29 to 37 (Fig. 4A). This motif probably corresponds to motif B of mouse Noxa, and the human *Noxa* gene lacks a DNA segment corresponding to the second exon of mouse *Noxa* (*9*). Human Noxa also induced apoptosis in various cells, including Saos2 cells in a BH3 motif–dependent manner (*9*). The promoter region of the human *Noxa* gene indeed contains one p53-response element (*9*), and increased expression of Noxa mRNA was observed in Saos2 cells infected with adenovirus encoding p53 (Fig. 4B). When an antisense oligonucleotide to Noxa was exposed in Saos2 cells, the increased expression of endogenous Noxa in response to p53 was inhibited, whereas control oligonucleotide had no effect (Fig. 4C) (*26*). Introduction of the antisense oligonucleotide also inhibited p53-induced apoptosis (Fig. 4D). Radiation-induced apoptosis in a hematopoietic cell line, BAF-3, is known to be dependent on p53 (*27*). Introduction of the antisense oligonucleotide to Noxa also inhibited the induction of Noxa expression and apoptosis (Fig. 4E). These results also support the notion that Noxa is a mediator of p53-induced apoptosis, at least in these assay systems.

Noxa may be an attractive candidate mediator of p53-mediated apoptotic response (*1*). It is likely that Noxa, and other p53 target genes, functionally cooperate with each other for the efficient induction of apoptosis in various cell types.

References and Notes

1. S. W. Lowe, *Curr. Opin. Oncol.* **7**, 547 (1995); T. M. Gottlieb and M. Oren, *Semin. Cancer Biol.* **8**, 359 (1998); T. F. Burns and W. S. El-Deiry, *J. Cell Physiol.* **181**, 231 (1999); R. V. Sionov and Y. Haupt, *Oncogene* **18**, 6145 (1999).
2. M. S. Soengas *et al.*, *Science* **284**, 156 (1999).
3. T. Miyashita and J. C. Reed, *Cell* **80**, 293 (1995).
4. C. M. Knudson, K. S. K. Tung, W. G. Tourtellotte, G. A. J. Brown, S. J. Korsmeyer, *Science* **270**, 96 (1995); M. E. McCurrach, T. M. Connor, C. M. Knudson, S. J. Korsmeyer, S. W. Lowe, *Proc. Natl. Acad. Sci. U.S.A.* **94**, 2345 (1997).
5. H. J. Brady, G. S. Salomons, R. C. Bobeldijk, A. J. Berns, *EMBO J.* **15**, 1221 (1996).
6. H. Nozawa *et al.*, *Genes Dev.* **13**, 1240 (1999); N. Tanaka *et al.*, *Cell* **77**, 829 (1994); N. Tanaka *et al.*, *Nature* **382**, 816 (1996).
7. P. Liang and A. B. Pardee, *Science* **257**, 967 (1992). For isolation of Noxa cDNA, the mRNA differential display method was performed with the mRNA Fingerprinting Kit (NipponGene, Tokyo). In this experiment, we cloned Noxa cDNA and two other previously unidentified genes regulated by p53 (R. Ohki, unpublished observation).
8. A. Gross, J. M. McDonnell, S. J. Korsmeyer, *Genes Dev.* **13**, 1899 (1999); J. M. Adams and S. Cory, *Science* **281**, 1322 (1998); A. Kelekar and C. B. Thompson, *Trends Cell Biol.* **8**, 324 (1998).
9. E. Oda and N. Tanaka, unpublished data.
10. Primary MEFs and mouse thymocytes were isolated and cultured as described (*6*). HeLa and Saos2 cells were cultured in Dulbecco's modified Eagle's medium supplemented with 10% fetal bovine serum. Total RNA was purified at various times after x-ray irradiation or p53-expressing adenovirus [S. Yamano *et al.*, *J. Virol.* **73**, 10095 (1999)] infection and subjected to RNA blot analysis as described (*6*).
11. S. W. Lowe, E. M. Schmitt, S. W. Smith, B. A. Osborne, T. Jacks, *Nature* **362**, 847 (1993); R. A. Clarke *et al.*, *Nature* **362**, 849 (1993).
12. Immunoblot analyses were done as described [A. Takaoka *et al.*, *EMBO J.* **18**, 2480 (1999)]. Antibody sources were as follows: monoclonal antibody to hemagglutinin (HA) (12CA5, Boehringer Mannheim), monoclonal antibody to cytochrome oxidase subunit IV (20E8-C12, Molecular Probes, Eugene, OR), monoclonal antibody to cytochrome c (7H8.2C12, BD Pharmingen, San Diego, CA), rabbit antibody to caspase-9 (BD Pharmingen), rabbit antibody to Bax (N-20, Santa Cruz Biotechnology, Santa Cruz, CA), rabbit antibody to Bcl-XL (S-18, Santa Cruz Biotechnology), and monoclonal antibody to Bcl-2 (6C8, BIOMOL Research Laboratories, Plymouth Meeting, PA). Rabbit antibodies to mouse and human Noxa were raised against synthetic peptides corresponding to amino acid residues 47 to 67 of mouse Noxa and 25 to 40 of human Noxa.
13. A mouse genomic library made from adult male liver DNA from strain C57BL/6N (CLONTECH, Palo Alto, CA) was screened with the Noxa cDNA as a probe, and cloned *Noxa* genomic DNA was sequenced up to 1 kb upstream from the first methionine codon. The exon-intron boundaries were determined by sequencing analysis. The transcription initiation site was determined by PCR-based primer extension analysis with a 5′ RACE system (CLONTECH).
14. A 329–base pair (bp) Sac II fragment containing the promoter and a potential p53-recognition sequence was inserted into the Picagene luciferase reporter plasmid (Wako, Osaka, Japan). Noxa-Δluc was constructed with a 286-bp Xho I to Sac II fragment (see Fig. 2A), and Noxa-mt-luc was constructed by the insertion of synthetic DNAs carrying the altered p53-recognition sequence [W. S. El-Deiry, S. E. Kern, J. A. Pietenpol, K. W. Kinzler, B. Vogelstein, *Nature Genet.* **1**, 45 (1992); H. Hermeking *et al.*, *Mol. Cell* **1**, 3 (1997)] into the Xho I site of Noxa-Δluc. For construction of the p53 expression vector (pEF-p53), human p53 cDNA was inserted into the pEF vector [S. Mizushima and S. Nagata, *Nucleic Acids Res.* **18**, 5322 (1990)]. Reporter constructs were cotransfected with pEF-p53 into $p53^{-/-}$ MEFs with lipofectAMINE PLUS (Life Technologies, Rockville, MD), and luciferase activity was measured as described (*7*).
15. Recombinant adenovirus was generated with pAxCAwt vector according to the manufacturer's protocol (Adenovirus Expression Vector Kit, Takara, Kyoto, Japan). Noxa cDNA and its derivatives were tagged with the sequence encoding 10 amino acids of influenza virus HA peptide at their NH_2-terminus. Noxa BH3 domain mutants were generated by a two-step PCR method with synthetic primers to introduce the first leucine (CTC) to alanine (GCC). Cells were infected with adenoviruses at multiplicity of infection of 250. Apoptosis was assessed by the TUNEL method using terminal deoxynucleotidyl transferase and fluorescein-dUTP as recommended by the manufacturer (Boehringer Mannheim). Apoptotic cells were counted with a FACScalibur (Becton-Dickinson).
16. J. Zha *et al.*, *J. Biol. Chem.* **272**, 24101 (1997).
17. E. Bossy-Wetzel, D. D. Newmeyer, D. R. Green, *EMBO J.* **17**, 37 (1998).
18. A. Gross, J. Jockel, M. C. Wei, S. J. Korsmeyer, *EMBO J.* **17**, 3878 (1998).
19. K. G. Wolter *et al.*, *J. Cell Biol.* **139**, 1281 (1997); A. Nechushtan, C. L. Smith, Y. T. Hsu, R. J. Youle, *EMBO J.* **18**, 2330 (1999).
20. J. Nemoto and E. Oda, unpublished observation.
21. H. Zou, W. J. Henzel, X. Liu, A. Lutschg, X. Wang, *Cell* **90**, 405 (1997); P. Li *et al.*, *Cell* **91**, 479 (1997); S. M. Srinivasula, M. Ahmad, T. Fernandes-Alnemri, E. S. Alnemri, *Mol. Cell* **1**, 949 (1998).
22. A. Hakem, T. Sasaki, I. Kozieradzki, J. M. Penninger, *J. Exp. Med.* **189**, 957 (1999); M. M. Sugrue, Y. Wang, H. J. Rideout, R. M. Chalmers-Redman, W. G. Tatton, *Biochem. Biophys. Res. Commun.* **261**, 123 (1999).
23. D. R. Green and J. C. Reed, *Science* **281**, 1309 (1998); M. G. Vander Heiden and C. B. Thompson, *Nature Cell Biol.* **1**, E209 (1999).
24. R. C. Marcellus, J. G. Teodoro, R. Charbonneau, G. C. Shore, P. E. Branton, *Cell Growth Differ.* **7**, 1643 (1996).
25. M. Hijikata, N. Kato, T. Sato, Y. Kagami, K. Shimotohno, *J. Virol.* **64**, 4632 (1990).
26. Phosphorothioate single-stranded oligonucleotides matching regions 157 to 176 of the human Noxa cDNA (APR, GenBank accession number D90070) sequence (5′-CATCTCCGCCGGTGCCGCCG-3′) were used as antisense, and its inverted sequence (5′-GCCGCCGTGGCCGCCTCTAC-3′) was used as a control; the same region of mouse Noxa cDNA sequence (5′-CATCTCAGAAACGCCGCGGC-3′) was used as antisense, and its inverted sequence (5′-CGGCGCCGCAAAGACTCTAC-3′) was used as control. These regions were synthesized

Nature **397**, 710 (1999)].
27. C. E. Canman, T. M. Gilmer, S. B. Coutts, M. B. Kastan, *Genes Dev.* **9**, 600 (1995); F. W. Quelle *et al.*, *Genes Dev.* **12**, 1099 (1998).
28. Single-letter abbreviations for the amino acid residues are as follows: A, Ala; C, Cys; D, Asp; E, Glu; F, Phe; G, Gly; I, Ile; K, Lys; L, Leu; M, Met; N, Asn; P, Pro; Q, Gln; R, Arg; S, Ser; T, Thr; V, Val; W, Trp; and Y, Tyr.
Oren, *Genes Dev.* **9**, 2170 (1995).
30. We thank M. Libonati, E. Barsoumian, G. Harris, H. Nozawa, H. Harada, Y. Saga, J. Inazawa, M. Emi, S. Taki, K. Ogasawara, M. Sato, A. Takaoka, H. Otsuka, K. Ishiodori, S. Hida, and T. Yokochi for invaluable advice and helpful discussions and N. Motoyama for human Bcl-XL cDNA. The mouse Noxa cDNA and its promoter sequences were deposited with GenBank (acces-

This work was supported in part by a special grant for advanced research on cancer from the Ministry of Education, Science, and Culture of Japan and by a research grant of the Princess Takamatsu Cancer Research Fund. E.O. and R.O. are research fellows of the Japan Society for the Promotion of Science.

13 January 2000; accepted 28 March 2000

Stable RNA/DNA Hybrids in the Mammalian Genome: Inducible Intermediates in Immunoglobulin Class Switch Recombination

Robert B. Tracy,[1] Chih-Lin Hsieh,[2,3] Michael R. Lieber[1,2,4,5]*

Although it is well established that mammalian class switch recombination is responsible for altering the class of immunoglobulins, the mechanistic details of the process have remained unclear. Here, we show that stable RNA/DNA hybrids form at class switch sequences in the mouse genome upon cytokine-specific stimulation of class switch in primary splenic B cells. The RNA hybridized to the switch DNA is transcribed in the physiological orientation. Mice that constitutively express an *Escherichia coli* ribonuclease H transgene show a marked reduction in RNA/DNA hybrid formation, an impaired ability to generate serum immunoglobulin G antibodies, and significant inhibition of class switch recombination in their splenic B cells. These data provide evidence that stable RNA/DNA hybrids exist in the mammalian nuclear genome, can serve as intermediates for physiologic processes, and are mechanistically important for efficient class switching in vivo.

Mammalian organisms require two types of DNA recombination to produce functional immunoglobulin (Ig) proteins. The first, called V(D)J recombination, mediates assembly of the variable domains of the Ig heavy and light chains in pre-B cells (*1*). Downstream of the V, D, and J segments is the region containing the Ig constant domains. In mice, this consists of eight distinct sets of constant domain exons (C_H), with the following organization: 5′-V(D)J-Cμ-Cδ-Cγ3-Cγ1-Cγ2b-Cγ2a-Cε-Cα-3′. In the second type of recombination, termed "class switch recombination" (CSR), the Cμ exons (and Cδ exons) are replaced by any one of the downstream C_H isotypes. This results in a deletion of the intervening genomic DNA as a circular product, which includes the Cμ exons (*2*). Replacement of Cμ ultimately causes a change from IgM to IgG, IgE, or IgA (*3–5*).

CSR from the IgM isotype to one or more of the downstream isotypes takes place anywhere within the several-kilobase G-rich (nontemplate strand) regions of repetitive DNA, termed "switch regions," which are located 5′ to each set of C_H exons (*6*). Immediately upstream of each mammalian switch region are intron promoters, which direct sterile transcripts into the switch and constant regions upon activation by particular cytokines (*4, 7*). Targeting of CSR to a given constant gene is considered to be tightly correlated with transcription from the corresponding upstream promoter (*3, 4, 8, 9*). Although the germ line transcripts appear to be required for CSR (*10, 11*) and in substrate studies (*12, 13*), their exact role in the targeting of class switch is unknown. Previous in vitro data showed stable RNA/DNA hybrid formation after transcription through switch sequences (*14, 15*). The RNA forms a hybrid with the DNA only when it is transcribed in the physiological direction (i.e., generation of G-rich RNA).

On the basis of this circumstantial evidence for RNA/DNA hybrid formation at switch sequences in vitro, we attempted to isolate RNA/DNA hybrids at several different murine switch sequences (Sμ, Sγ3, Sγ1, Sγ2b, Sε, and Sα) in the genome of B cells that are actively undergoing CSR [see supplementary Web material (*16*) for details]. The experimental design involved (i) enriching for small resting B cells from the spleens of wild-type C57Bl/6 mice, (ii) inducing the cells to undergo CSR by adding lipopolysaccharide (LPS) and appropriate cytokines, (iii) allowing the cells to proliferate for 2.5 days, (iv) isolating the genomic DNA, (v) treating the DNA with an excess of ribonuclease (RNase) A, and (vi) digesting all of the genomic DNA with deoxyribonuclease I. At this stage, the only nucleic acid remaining should be RNA that was stably hybridized to genomic DNA and, hence, protected from RNase A treatment.

Initially, we attempted to detect RNA/DNA hybrids at Sμ and Sγ3 by reverse transcription–polymerase chain reaction (RT-PCR) on RNA purified from B cells stimulated with LPS and interleukin-10 (IL-10) (*17*). When we examined the 5′ end of Sμ and Sγ3, we found that an RT-PCR product of the correct size is generated from an RNase A–resistant RNA species at both loci (Fig. 1B, lanes 1 and 4, respectively). The RNA species is also present at the 3′ end of Sγ3, as evidenced by the generation of the correct-sized RT-PCR product (Fig. 1B, lane 7). Lanes 3 and 6 show that these bands are undetectable in the absence of RT, eliminating the possibility that the observed PCR product is a consequence of genomic DNA contamination (Fig. 1B). To confirm that the RNA is involved in hybrid formation, we treated the genomic DNA with RNase H (which only hydrolyzes RNA involved in hybrid formation) and RNase A simultaneously. Upon treatment with RNase H, the RT-PCR products disappear (Fig. 1B, lanes 2, 5, and 8).

To confirm that RNA/DNA hybrid formation is a general property of mouse switch sequences, we examined hybrid formation at Sγ1 and Sε following stimulation of the B cells with IL-4 rather than IL-10. RT-PCR products of the expected sizes were produced in the absence (lanes 9 and 11) but not in the presence of RNase H (lanes 10 and 12) (Fig. 1B), thus confirming the presence of a hybrid at these sequences. For Sμ, Sγ3, and Sγ1, we verified that the RNA in the hybrid was the G-rich RNA being generated in the physiologic direction by performing RT-PCR with strand-specific primers during RT (RBT49, RBT08, and RBT14 in Fig. 1A) [see Web fig. 1 (*16*)].

To confirm the RT-PCR data, we attempted to detect hybrid formation at the Sμ and Sγ3 genomic loci by Northern blot analysis (Fig. 2) (*18*). As a positive control, we tried to detect germ line transcripts by Northern blot

[1]Department of Pathology, [2]Department of Biochemistry and Molecular Biology, [3]Department of Urology, [4]Department of Microbiology, [5]Department of Biology, University of Southern California Keck School of Medicine, Norris Comprehensive Cancer Center, Rooms 5420 and 5428, Los Angeles, CA 90089–9176, USA.

*To whom correspondence should be addressed. E-mail: lieber@hsc.usc.edu